LLNL-TR-410557

LAWRENCE
LIVERMORE
NATIONAL
LABORATORY

Predicted neutron yield and radioactivity for laser-induced (p,n) reactions in LiF

D. C. Swift, J. M. McNaney

February 13, 2009

Disclaimer

This work performed under the auspices of the U.S. Department of Energy by Lawrence Livermore National Laboratory under Contract DE-AC52-07NA27344.

Predicted neutron yield and radioactivity for laser-induced (p,n) reactions in LiF

Damian C. Swift and James M. McNaney
PLS-CMMD, Lawrence Livermore National Laboratory,
7000 East Avenue, Livermore, California 94550, USA
(Dated: January 30, 2009)

Design calculations are presented for a pulsed neutron source comprising polychromatic protons accelerated from a metal foil by a short-pulse laser, and a LiF converter in which (p,n) reactions occur. Although the proton pulse is directional, neutrons are predicted to be emitted relatively isotropically. The neutron spectrum was predicted to be similar to the proton spectrum, but with more neutrons of low energy in the opposite direction to the incident protons. The angular dependence of spectrum and intensity was predicted. The (p,n) reactions generate unstable nuclei which decay predominantly by positron emission to the original ^{7}Li and ^{19}F isotopes.

For the initial planned experiments using a converter 1 mm thick, we predict that 0.1% of the protons will undergo a (p,n) reaction, producing 10^9 neutrons. Ignoring the unreacted protons, neutrons, and prompt gamma emission as excited nuclear states decay, residual positron radioactivity (and production of pairs of 511 keV annihilation photons) is initially 4.2 MBq decaying with a half-life of 17.22 s for 6 mins (^{19}Ne decays), then 135 Bq decaying with a half-life of 53.22 days (^{7}Be decays).

PACS numbers: 07.35.+k, 52.38.Mf, 47.40.Nm, 79.20.Ds
Keywords: accelerator, ultrashort laser pulse, nuclear physics, proton-neutron reaction

I. INTRODUCTION

We have proposed to use (p,n) reactions as a source of neutrons for temperature measurements *in-situ* during shock loading. The protons would be generated by the interaction of an intense laser pulse with a thin foil [1–3], and temperature would be deduced using neutron resonance spectrometry (NRS) [4]. It is important to optimize the yield and spectrum of neutrons from the (p,n) target to the shock experiment. Most recent research in laser-based ion acceleration has concentrated on increasing the ion energy into the hundreds of MeV to GeV range, for applications in thermonuclear fast ignition. These energies are inconveniently high for our NRS applications; also it is likely that the proton yield would be much greater at low energies. We are planning a series of experiments to measure and optimize laser-accelerated protons in the few to tens of MeV range. Here we present predictions of neutron yield and spectrum, and of residual radioactivity from the (p,n) target, for our initial experiments using LiF, for detector design and safety purposes.

II. PROTON SPECTRUM

Several groups have reported measurements of proton spectra from short-pulse laser experiments [2, 3, 5], which have been similar though with significant variations. Typically, the proton spectrum is broadband from ∼1 MeV to several tens of MeV. At low energies, the measurements typically lose resolution, and it is possible that large numbers of sub-MeV protons are generated. Our experiments are planned for the Titan system at Lawrence Livermore National Laboratory's Jupiter Laser Facility [6], so we have taken a spectrum measured on that specific system: a Boltzmann distribution with a temperature of 2.5 MeV [2] (Fig. 1).

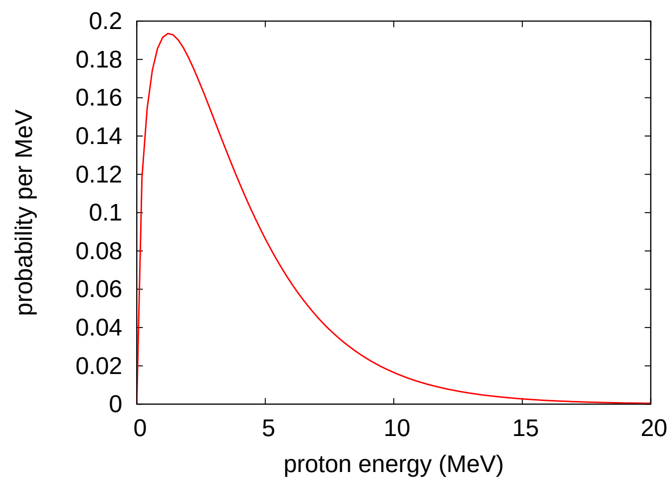

FIG. 1: Probability distribution of kinetic energy for protons at an effective temperature of 2.5 MeV.

Measured yields are $\sim 10^{12}$ protons per pulse, a number which is similar on at least three different laser systems [2, 3, 5].

III. NEUTRON YIELD

For our initial experiments, the (p,n) converter material chosen was LiF, as it is readily available, has low cost, is conveniently in solid form, and is relatively non-hazardous. It is not the substance expected to give the

TABLE I: Isotopes in LiF.

isotope	abundance (at. %)
^{7}Li	92.5
^{6}Li	7.5
^{19}F	100

TABLE II: (p,n) reaction energetics in LiF.

isotope	energy released, Q (MeV)	CM threshold energy (MeV)	proton threshold energy (MeV)
^{7}Li	-1.644	1.880	2.456
^{6}Li	-5.071	5.920	8.058
^{19}F	-4.021	4.234	4.691

beat possible neutron yield. Li occurs in two stable isotopes of atomic weight 6 and 7. The relative abundance depends on the source of the Li; for the present study we assumed average terrestrial abundances (Table I). Both isotopes of Li undergo (p,n) reactions, though ^{6}Li has a significantly higher threshold energy. ^{19}F, the only stable isotope, also undergoes (p,n) reactions, though with a higher threshold energy than for ^{7}Li.

A. Energetics

Energetics for the (p,n) reactions were taken from the Atomic Mass Data Center [7] (Table II).

B. Cross-sections

Reaction cross-section data were taken from the ENDF library [8]. For ^{7}Li, (p,n) cross-sections have been measured in detail up to $\sim$4 MeV, and with successively coarser energy resolution up to $\sim$25 and $\sim$200 MeV. For ^{6}Li, no (p,n) cross-sections were reported; the interaction is more likely to result in ^{3}He and ^{4}He being produced. For ^{19}F, (p,n) cross-sections have been measured in detail up to $\sim$7 MeV, and sparsely up to $\sim$30 MeV. (Figs 2 and 3).

Protons with a Maxwellian energy distribution should couple efficiently to ^{7}Li(p,n): $\sim$90% of the protons have a kinetic energy below 8 MeV, where the cross-section is greatest. Around 20% of the protons are above 6 MeV, where ^{19}F(p,n) reactions can take place.

The mass density of LiF is 2.638 g/cm^3 [9], so the density of both Li and F atoms is 6.11×10^{28}/m^3. Ignoring competing interactions, we can estimate a mean cross-section for the (p,n) reactions and hence estimate a mean

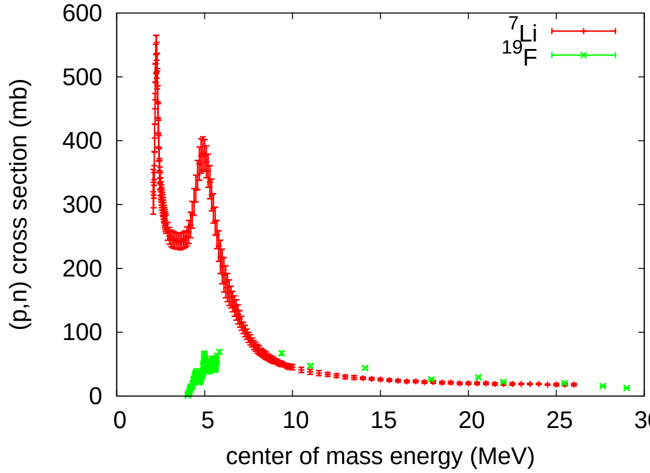

FIG. 2: (p,n) cross-sections for ^{7}Li and ^{19}F.

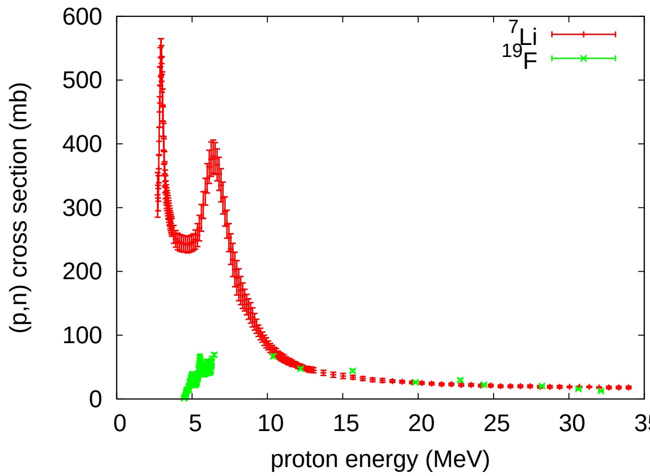

FIG. 3: (p,n) cross-sections for ^{7}Li and ^{19}F, plotted with respect to proton energy for target nuclei at rest.

conversion length (distance for $1/e$ of the protons to react) for Li and F in turn, and hence for LiF (Table III).

Again neglecting competing reactions, the approximate yield of neutrons is

$$N_n \simeq N_p \left(1 - e^{-l_t/l_c}\right) \tag{1}$$

where N_p is the number of protons, l_c the conversion length, and l_t the target thickness. In early experiments, we will be conservative in the efficiency of neutron generation to reduce the risk of radiation exposure. For targets that are much thinner than the conversion length,

$$N_n \simeq N_p \frac{l}{l_c}. \tag{2}$$

TABLE III: Representative cross-sections and conversion lengths for (p,n) reactions in $^{7}Li^{19}F$.

species	mean (p,n) cross-section (millibarns)	conversion length (m)
^{7}Li	200	0.82
^{19}F	30	5.46
$^{7}Li^{19}F$		0.71

TABLE IV: Representative cross-sections and conversion lengths ($1/e$) for neutron scattering and absorption LiF.

species	scattering length (m)	absorption length (m)
Li	0.16	0.16
F	0.05	3.27
LiF	0.04	0.16

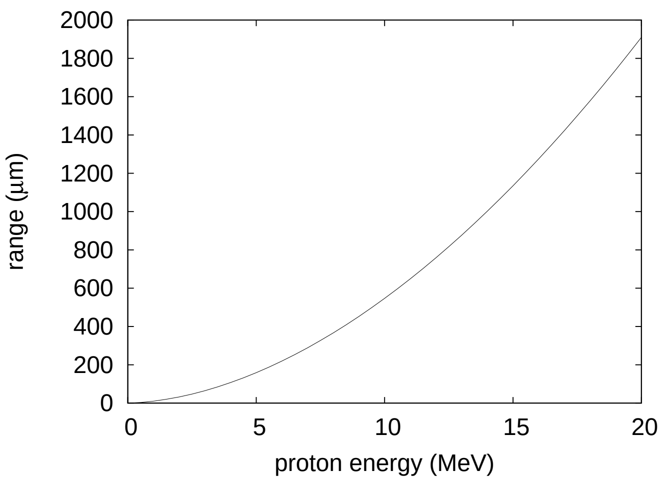

FIG. 4: Approximate range of protons in LiF.

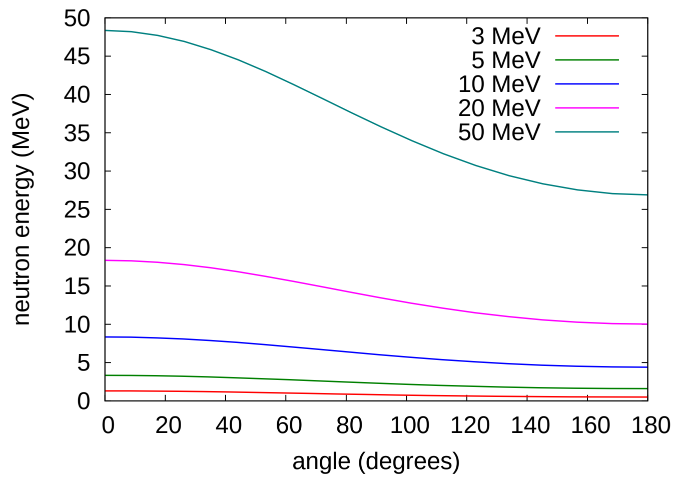

FIG. 5: Predicted neutron energy from monoenergetic protons as a function of angle from the incident proton beam, for ^{7}Li(p,n).

C. Proton range

As the protons traverse the converter, they lose kinetic energy to nuclei and electrons, and eventually become too slow for any of the (p,n) reactions to take place. Here we estimate the proton range, to account for proton stopping in calculating the number of protons available to take part in (p,n) reactions. An analytic solution [10] to the Bethe ion stopping relation [11] was used, which should be ∼1% accurate in the regime of interest. The Bethe relation holds for elements. The stopping power of Li and F together was calculated using the Bragg additive estimate. For each target specie, the Bloch estimate [12] was used for its ionization,

$$\bar{I} \simeq 10Zq, \tag{3}$$

where Z is the atomic number of the specie. (Fig. 4)

D. Neutron range

The efficiency of the converter is reduced by absorption of the neutrons produced. Relevant interactions include inelastic scattering and nuclear reactions. Reaction cross-section data were taken from the ENDF library [8]. For ^{6}Li and ^{7}Li, representative cross-sections in the energy range of interest are ∼1 b each for scattering and reactions, with reactions dominated by ^{2}H and ^{3}H formation. For ^{19}F, the scattering is dominant at ∼2-3 b (mostly elastic), and the most significant reaction is (n,α) at ∼0.05 b. The capture and scattering of neutrons can thus be related to intensity and spectrum produced (Table IV).

IV. NEUTRON SPECTRUM

For a given proton energy, kinematics was used to estimate the energy of the neutron as a function of angle from the direction of the proton, using a derivation and software implementation tested against relevant experimental data on neutron generation [13] (Figs 5 and 6). This is an overestimate of the neutron energy, as it is possible for the product nuclide to be left in an excited state. The systematic trends can be represented more clearly by comparing the neutron energy with the energy of the incident proton (Figs 7 and 8), and are captured compactly by comparing with the proton energy once the (endothermic) reaction energy has been taken into account (Figs 9 and 10).

Next we calculate the angle-dependent spectrum, ignoring the effects of deceleration and absorption of

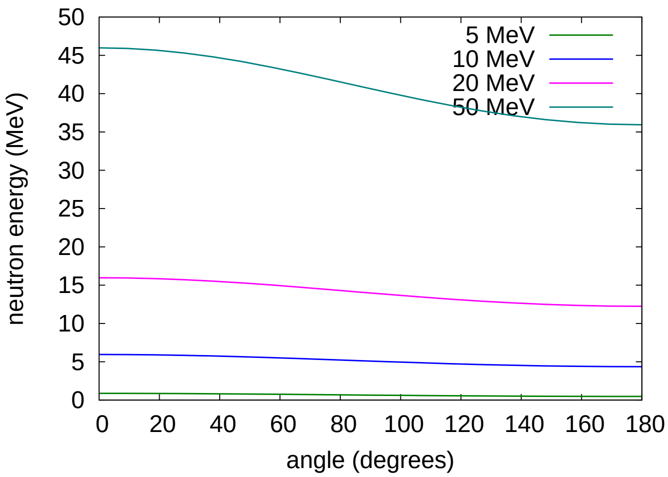

FIG. 6: Predicted neutron energy from monoenergetic protons as a function of angle from the incident proton beam, for ^{19}F(p,n).

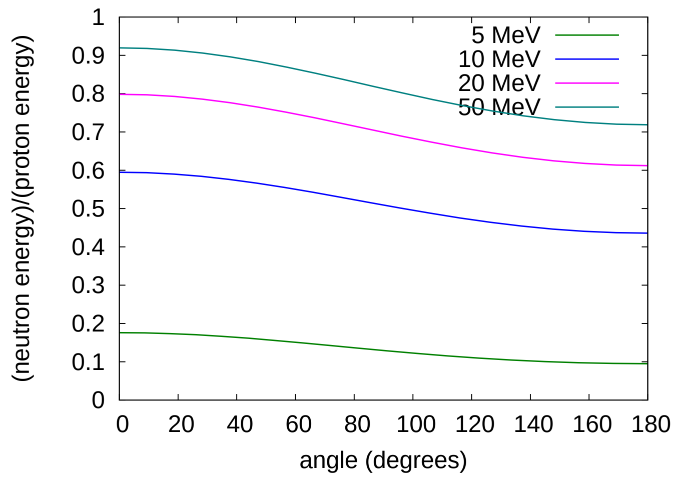

FIG. 8: Predicted neutron energy from monoenergetic protons as a function of angle from the incident proton beam, for ^{19}F(p,n), expressed as the ratio between the neutron and proton energies.

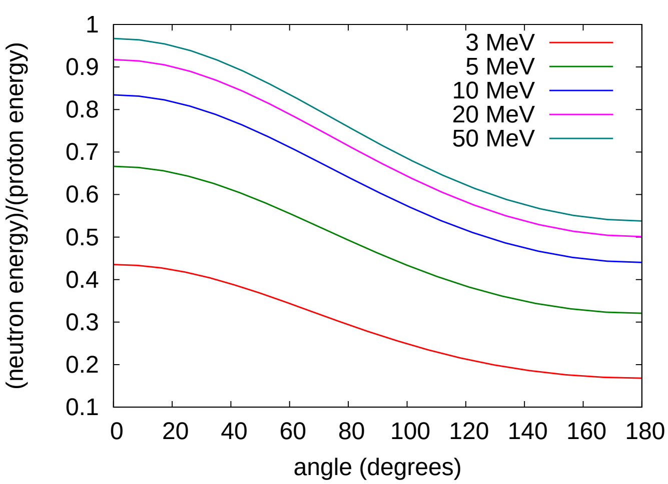

FIG. 7: Predicted neutron energy from monoenergetic protons as a function of angle from the incident proton beam, for ^{7}Li(p,n), expressed as the ratio between the neutron and proton energies.

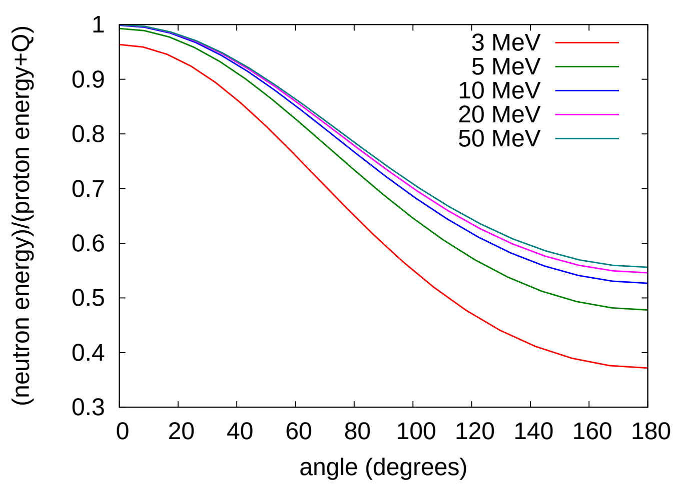

FIG. 9: Predicted neutron energy from monoenergetic protons as a function of angle from the incident proton beam, for ^{7}Li(p,n), expressed as the ratio between the neutron and residual proton energies.

protons. A numerical integration was performed over the proton spectrum (including energy-dependent cross-sections) and the neutron angle, collected as a distribution over discrete bins. For the initial experiments, we plan to use LiF 1 mm thick. The calculations predicted a yield of 10^{-3} neutrons per proton. The effect of scattering and absorption of the neutrons within the LiF should be only a small perturbation. 89.5% of the reactions were with ^{7}Li. (Figs 11 to 14.)

Spectra were also calculated at 140° from the proton beam, where diagnostics will be located (Figs 15 and 16).

V. RADIOACTIVITY

The (p,n) reactions

$$^{7}\mathrm{Li} + p \;\rightarrow^{7}\mathrm{Be} + n \quad \text{(-1.644 MeV)} \tag{4}$$
$$^{19}\mathrm{F} + p \;\rightarrow^{19}\mathrm{Ne} + n \quad \text{(-15.291 MeV)} \tag{5}$$
$$\tag{6}$$

produce unstable product nuclei. The decay modes and resulting radioactivity were assessed using the NuDat database [14].

In the case of ^{7}Be, excited states in the likely range

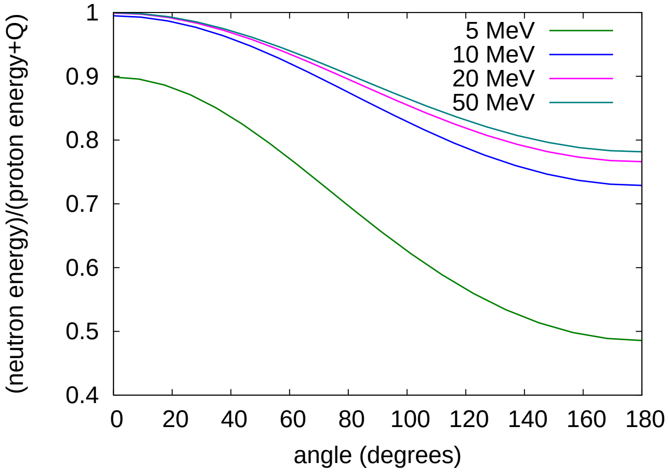

FIG. 10: Predicted neutron energy from monoenergetic protons as a function of angle from the incident proton beam, for ^{19}F(p,n), expressed as the ratio between the neutron and residual proton energies.

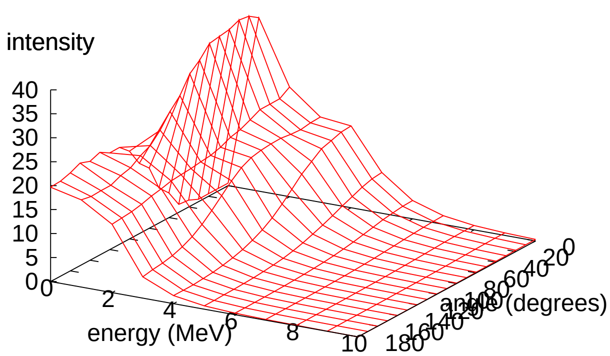

FIG. 11: Predicted neutron spectrum as a function of angle for a Boltzmann distribution of incident protons with characteristic temperature 2.5 MeV and 1 mm of LiF. The angle is with respect to the proton beam, and the intensity is in neutrons/(MeV.sr) per 10^6 protons.

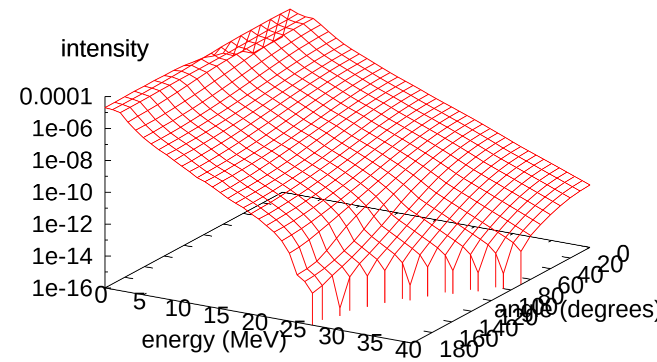

FIG. 12: As for Fig. 11 but log scale and intensity is in neutrons/(MeV.sr) per incident proton.

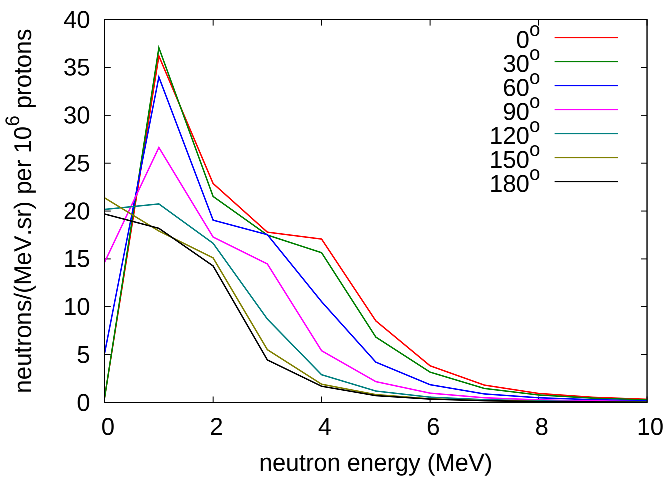

FIG. 13: Predicted neutron spectrum as a function of angle for a Boltzmann distribution of incident protons with characteristic temperature 2.5 MeV and 1 mm of LiF. The angle is with respect to the proton beam.

of energies (∼MeV) decay rapidly by gamma emission. The ground state undergoes β^+ decay back to ^{7}Li, with a half-life of 53.22 days. Radioactivity is in the form of γ radiation of a few hundred keV to a few MeV from the decay of the excited state, then positrons and resulting annihilation gammas at 511 keV (two per decay).

For ^{19}Ne, the ground state decays by β^+ emission back to ^{19}F, with a half-life of 17.22 s. There may be γ radiation from the decay of excited nuclear states. 0.09% of the β decay is in the form of Auger electrons at 0.66 keV, but positron emission predominates, resulting in two gammas of 511 keV from annihilation of each positron, and ∼1.5 MeV gammas with a low intensity.

For the expected yield from the initial experiments, with an estimated 10^9 neutrons produced, the induced radioactivity would be 4.2 MBq initially, dominated by the decay of ^{19}Ne. After 6 mins, enough of the ^{19}Ne has decayed that the radioactivity is now dominated by decay of the ^{7}Be, with an activity of 135 Bq (Fig. 17). These calculations ignore the neutrons themselves, unreacted protons, and prompt gammas from the decay of excited nuclear states.

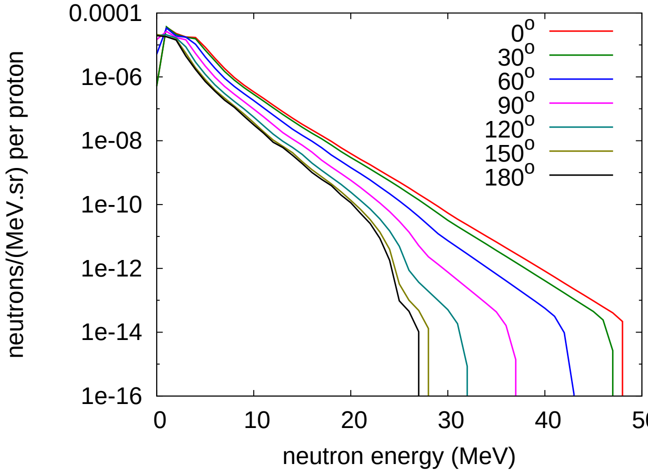

FIG. 14: As for Fig. 13 but log scale.

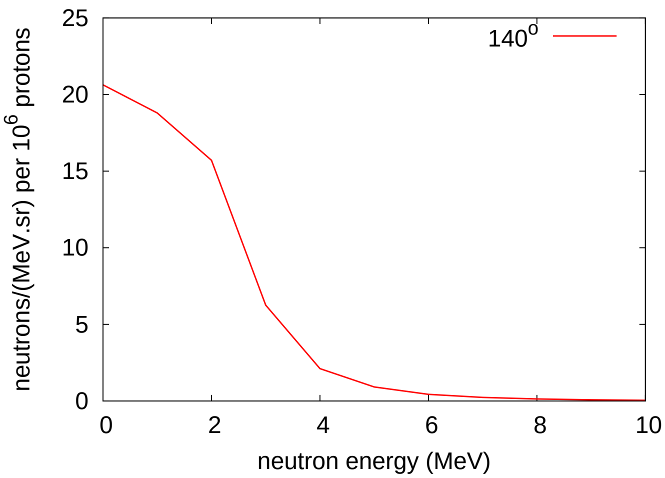

FIG. 15: Predicted neutron spectrum at 140° for a Boltzmann distribution of incident protons with characteristic temperature 2.5 MeV and 1 mm of LiF.

VI. CONCLUSIONS

The expected yield from a short-pulse high-energy laser, 10^{12} protons, directed into a converter comprising 1 mm thick LiF, should produce 10^9 neutrons, ignoring deceleration of the protons. The spectrum was predicted to vary significantly with angle, more numerous and faster neutrons being directed parallel with the incident protons, and a greater number of sub-MeV neutrons in the backward direction.

Apart from the neutrons and prompt gammas of hundreds of keV to a few MeV, induced radioactivity is dominated by β^+ radiation from decay of the isotope produced from each captured proton, generating pairs of 511 keV gammas on annihilation within the LiF or its surroundings. For the anticipated trial experiments with 10^9 neu-

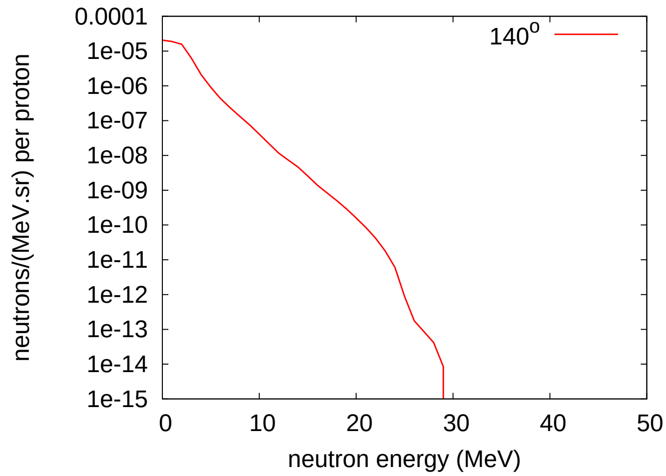

FIG. 16: As for Fig. 15 but log scale.

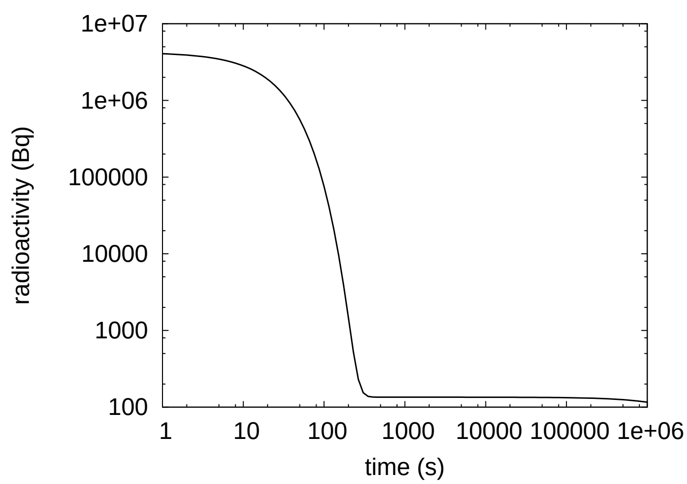

FIG. 17: Predicted radioactivity from 1 mm thick LiF target. Note that 10^6 s is approximately 11.6 days.

trons This residual radioactivity is initially 4.2 Bq, decaying with a half-life of 17.22 s; after 6 mins, it is 135 Bq, decaying with a half-life of 53.22 days. The unstable nuclei decay back to ^{7}Li and ^{19}F, so the composition of the converter does not age significantly.

[1] S.P. Hatchett, C.G. Brown, T.E. Cowan, E.A. Henry, J.S. Johnson, M.H. Key, J.A. Koch, A.B. Langdon,

B.F. Lasinski, R.W. Lee, A.J. Mackinnon, D.M. Pennington, M.D. Perry, T.W. Phillips, M. Roth, T.C. Sangster, M.S. Singh, R.A. Snavely, M.A. Stoyer, S.C. Wilks, and K. Yasuike, Phys. Plasmas **7**, 2076 (2000).

[2] A.J. Mackinnon, Y. Sentoku, P.K. Patel, D.W. Price, S. Hatchett, M.H. Key, C. Andersen, R. Snavely, and R.R. Freeman, Phys. Rev. Lett. **88**, 215006 (2002).

[3] K. Flippo, B.M. Hegelich, B.J. Albright, L. Yin, D.C. Gautier, S. Letzring, M. Schollmeier, J. Schreiber, R. Schulze, and J.C. Fernandez, Laser and Particle Beams **25**, 3-8 (2007).

[4] V.W. Yuan, J.D. Bowman, D.J. Funk, G.L. Morgan, R.L. Rabie, C.E. Ragan, J.P. Quintana, and H.L. Stacy, Phys. Rev. Lett. **94**, 125504 (2005).

[5] M.J. Rubery, A.J. Simons, M. Gardner, P.C. Thompson, *Proton activation experiments at HELEN*, Plasma Physics Department Annual Report 2007 pp 97-99 (AWE, Reading, 2007).

[6] B.C. Stuart, J.D. Bonlie, J.A. Britten, J.A. Caird, R. Cross, C.A. Ebbers, M.J. Eckart, A.C. Erlandson, W.A. Molander, A. Ng, P. Patel, and D.F. Price, Proc. Conf. on Lasers and Electro-Optics (CLEO), Long Beach, Ca, USA, May 21, 2006, paper JTuG3 (Optical Society of America, 2006).

[7] A.H. Wapstra, G. Audi, and C. Thibault, Nuc. Phys. A **729**, 129 (2003); G. Audi, A.H. Wapstra, and C. Thibault, Nuc. Phys. A **729**, 337 (2003).

[8] M.B. Chadwick, P. Obložinský, M. Herman, N.M. Greene, R.D. McKnight, D.L. Smith, P.G. Young, R.E. MacFarlane, G.M. Hale, S.C. Frankle, A.C. Kahler, T. Kawano, R.C. Little, D.G. Madland, P. Moller, R.D. Mosteller, P.R. Page, P. Talou, H. Trellue, M.C. White, W.B. Wilson, R. Arcilla, C.L.Dunford, S.F. Mughabghab, B. Pritychenko, D. Rochman, A.A. Sonzogni, C.R. Lubitz, T.H. Trumbull, J.P. Weinman, D.A. Brown, D.E. Cullen, D.P. Heinrichs, D.P. McNabb, H. Derrien, M.E. Dunn, N.M. Larson, L.C. Leal, A.D. Carlson, R.C. Block, J.B. Briggs, E.T. Cheng, H.C. Huria, M.L. Zerkle, K.S. Kozier, A. Courcelle, V. Pronyaev and S.C. van der Marck, Nuclear Data Sheets **107**, pp 2931-3060 (2006).

[9] D.J. Steinberg, *Equation of state and strength parameters for selected materials*, Lawrence Livermore National Laboratory report UCRL-MA-106439 change 1 (1996).

[10] D.C. Swift and J.M. McNaney, *Approximate, analytic solutions of the Bethe equation for charged particle range*, preprint `arXiv:0901.4145` (2009).

[11] H. Bethe, Ann. Phys. **397**, 3, pp 325-400 (1930).

[12] F. Bloch, Ann. Phys. **16**, 287 (1933).

[13] D.C. Swift and J.M. McNaney, *Calculation of neutron energy versus angle for beam-target reactions*, Lawrence Livermore National Laboratory report XXXX (2008).

[14] NuDat 2 database, Brookhaven National Laboratory, January 2009.